Acta Crystallographica Section C
Crystal Structure Communications
ISSN 0108-2701

Differently coloured polymorphs of 4-[(2-nitrophenyl)azo]phenol

Alexandr V. Yatsenko* and Ksenia A. Paseshnichenko

Chemistry Department, Moscow State University, 119899 Moscow, Russia
Correspondence e-mail: yatsenko@biocryst.phys.msu.su

Received 10 April 2001
Accepted 8 May 2001

The crystal structures of the brown–yellow and orange polymorphs of the title compound, 4-[(2-nitrophenyl)-diazenyl]phenol, $C_{12}H_9N_3O_3$, have been determined and their visible reflection spectra recorded. Both structures adopt a stacking arrangement with interstack hydrogen bonds. *Ab initio* and semi-empirical (*AM*1 and *INDO-CISD*) calculations were performed in order to rationalize the difference in colour. It can be attributed neither to the subtle distinctions in molecular geometry nor to the effect of intermolecular electrostatic interactions. The most probable origin of this difference is the mixing of intramolecular $n \rightarrow \pi^*$ and intermolecular charge-transfer excitations.

Comment

The first examples of differently coloured crystalline forms of organic compounds were reported 94 years ago (Hantzsch, 1907). This phenomenon was originally called chromo-isomerism, but recently the more appropriate term crystallo-chromy has been introduced (Klebe *et al.*, 1989). The current version of the Cambridge Structural Database (CSD; Allen & Kennard, 1993) contains more than 50 families of differently coloured polymorphs and pseudopolymorphs, but for only a few of them have the solid-state spectra been reported and the distinctions in colour rationalized.

These distinctions may be of various natures. Firstly, the molecules in the crystals may exist as different tautomeric forms or may adopt different conformations. In this case, the difference in colour can be interpreted at the level of the calculated electronic spectra of these tautomers or conformers. Secondly, the shifts of the absorption bands may arise from the perturbation of molecular orbitals (MOs) under the effect of the crystal environment. This effect is closely related in its nature to solvatochromism and can be modelled *via* incorporation of the external electrostatic potential into the Hamiltonian of a molecule (Csikós *et al.*, 1999; Yatsenko & Paseshnichenko, 2000). Thirdly, the absorption bands may be shifted and split due to the collective interactions within the crystals upon excitation. These effects can be considered at the level of the exciton–polariton approach (Philpott, 1971) and they are very large for strongly allowed transitions in some organic dyes, but are shadowed by other effects for moderately absorbing crystals. Fourthly, the bands corresponding to the intermolecular charge-transfer (CT) interaction can appear not only in the crystals with interlaced donor and acceptor molecules, but also in homomolecular crystals (Sebastian *et al.*, 1981). If the intermolecular π interactions are strong, the excitonic and CT states mix and should be considered together within the general theory (Hoffmann *et al.*, 2000). In order to extend the understanding of these various factors, we have studied 4-[(2-nitrophenyl)azo]phenol, (I), and present its crystal structure here.

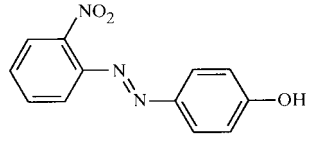

(I*a*), (I*b*)

As shown in Fig. 1, the electronic spectrum of (I) in CCl_4 solution is typical of azophenols (Okawara *et al.*, 1988). It contains a medium–strong absorption band in the near UV and a weak maximum in the visible region, attributed to the $\pi \rightarrow \pi^*$ and the $n \rightarrow \pi^*$ excitations, respectively. Fig. 1 indicates that the polymorphs (I*a*) and (I*b*) differ in colour due to the different intensity of the $n\pi^*$ band in their solid-state reflection spectra, because the red and yellow hues of coloured materials arise from the absorbance at 20 000 and above 23 000 cm^{-1}, respectively (Griffiths, 1976). The yellow and orange forms of 1,1′-dinitro-3,3′-azo-1,2,4-triazole (Cromer *et al.*, 1988) provide another example of polymorphs whose colour arises from the $n \rightarrow \pi^*$ excitation.

The bond lengths and angles in both structures are within the normally expected ranges. The molecular conformations in (I*a*) and (I*b*) differ; in (I*a*), the two rings attached to the azo linkage are twisted to the same side and are thus essentially coplanar, whereas in (I*b*), the rings are rotated opposite to each other (Table 1). The two independent molecules in (I*b*)

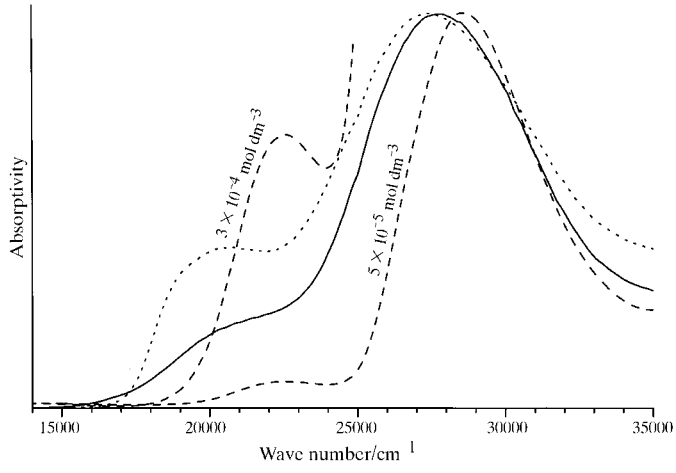

Figure 1
The absorption spectra of (I). Dashed lines: solution in CCl_4 at two different concentrations; solid line: reflection spectrum of (I*a*); dotted line: reflection spectrum of (I*b*).

form pseudo-centrosymmetric pairs and adopt essentially the same conformation. The twist of the nitro group out of the plane of the phenyl ring results from the compromise between N···O repulsion and π-delocalization. Overall, the molecule of (I*a*) is slightly flattened with respect to (I*b*).

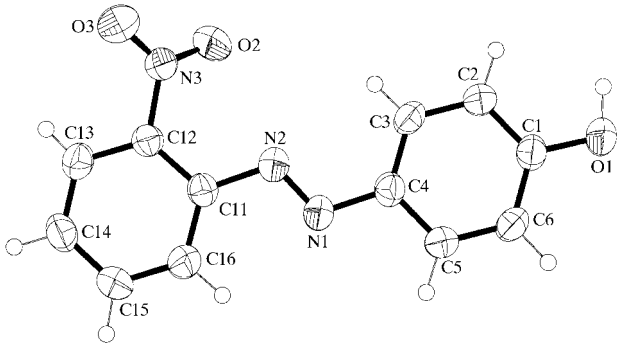

Figure 2
The asymmetric unit of (I*a*) with 50% probability displacement ellipsoids and the atom-numbering scheme. H atoms are drawn as small spheres of arbitrary radii.

The molecules in (I*a*) form stacks along [010]. The shortest intermolecular C···C distances are 3.536 (3) Å and neighbouring molecules within the stack are related by inversion centres. In (I*b*), neighbouring molecules are related by the [100] translation, and the shortest C···C distances within the stack are 3.478 (6) Å. The molecules are linked *via* hydrogen bonds, to form dimers in (I*a*) and tetramers in (I*b*) (Fig. 4 and Table 2), and the two independent molecules in (I*b*) are non-equivalent in the hydrogen-bonding pattern.

In order to compare the molecular electronic structures in (I*a*) and (I*b*), and to determine the effect of crystal packing, we have carried out semi-empirical calculations at the *AM*1 level (Dewar *et al.*, 1985), with the experimental molecular geometries used as input for the calculations. The molecular dipole moment in (I) is determined by the contributions of the nitro group and the hydroxy oxygen lone pair, and it is nearly perpendicular to the long axis of the molecule. Intermolecular interactions therefore cause only a subtle increase (0.03–0.05 e) in the intramolecular CT from the phenolic moiety to the nitro-substituted ring.

Under the effect of the crystal electrostatic potential, the gap between the highest occupied molecular orbital (HOMO) and the lowest unoccupied molecular orbital (LUMO) decreases from 7.79 to 7.61 eV in (I*a*) and from 7.91 to 7.58 eV in (I*b*), but in (I*b*), the LUMO and HOMO are localized on molecules 1 and 2, respectively. Such non-equivalence is caused by the hydrogen bonding: since the orbitals of the hydroxy O atom make a significant contribution to HOMO, this MO can be stabilized or destabilized by hydrogen bonds formed *via* the H or O atom of this group, respectively. Had the hydrogen bonds been formed *via* the azo N atoms, as in the structure of 4-(phenyldiazenyl)naphthalen-1-amine (Yatsenko *et al.*, 2001), their impact on the molecular electronic structure would have been much more pronounced, because the azo linkage makes a much larger contribution to the LUMO than the nitro group.

On transfer from aliphatic to aromatic azo compounds, the intensity of the $n \rightarrow \pi^*$ transition increases due to the interaction between the azo nitrogen lone pairs and the aromatic π systems, which is assisted by the deviation of a molecule from planarity (Griffiths, 1976). We studied the effect of the conformerism of (I) on the electronic spectra at the *INDO-CISD* level. In its original parameterization (Dick & Nickel, 1983), this method strongly underestimates the energy and intensity of the $n \rightarrow \pi^*$ transition. For (I), the calculations predict a gap of 14 000 cm^{-1} between the $n\pi^*$ and $\pi\pi^*$ excited states, whereas the experimentally determined value is about 6000 cm^{-1}. Similarly, the observed oscillator strength estimated according to Guillaumont & Nakamura (2000) is 0.018, *versus* 0.0009 obtained from the calculations. The structures of the molecular orbitals calculated using *INDO-CISD* differ from those obtained in the *ab initio* calculations. Since *INDO* overestimates the energy of the MO, which is mainly composed of the nitrogen 'lone-pair' atomic orbitals, by *ca* 1.4 eV, this orbital is HOMO-1 in the *INDO* calculations, but

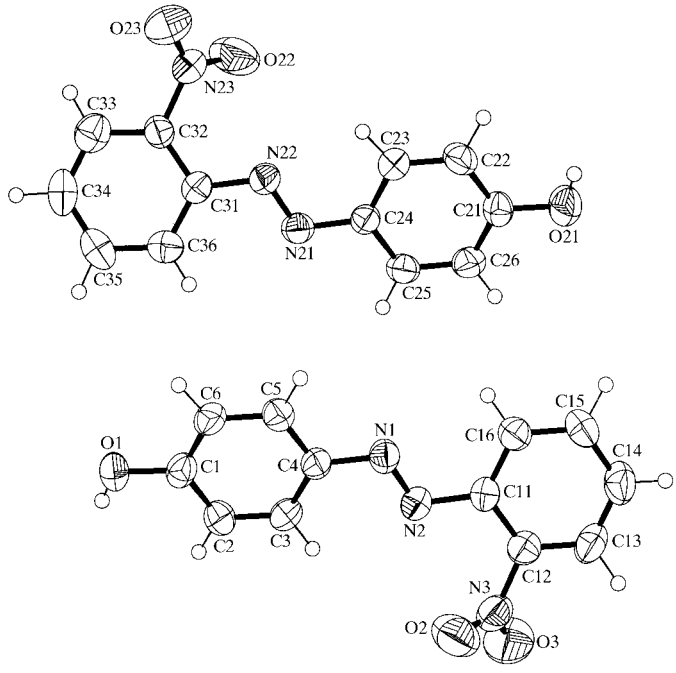

Figure 3
The asymmetric unit of (I*b*) with 50% probability displacement ellipsoids and the atom-numbering scheme. H atoms are drawn as small spheres of arbitrary radii. Atoms O1–C16 belong to molecule 1 and atoms O21–C36 belong to molecule 2.

only HOMO-4 according to the *ab initio* results. Following Ridley & Zerner (1973), we have introduced into the *INDO-CISD* scheme an additional empirical parameter f_σ (equal to 1.2) for scaling up the σ–σ overlap integrals. Besides this, we have increased both core integrals for the N atom by 9%. With these modifications, the *INDO*-calculated MOs match quite well with those obtained in the *ab initio* calculations, and the calculated $n\pi^*$–$\pi\pi^*$ gap and the oscillator strength for the $n \rightarrow \pi^*$ transition are in much better agreement with the experimental data.

Calculations on isolated molecules showed that the difference in molecular geometry between (I*a*) and (I*b*) is not enough to explain the observed spectral distinctions of these polymorphs. The $n \rightarrow \pi^*$ oscillator strength in (I*a*) was even calculated to be slightly larger than in (I*b*) [0.007 in (I*a*) *versus* 0.004 and 0.006 in the two molecules of (I*b*)]. With the crystal electrostatic potential applied, *INDO-CISD* predicts a bathochromic shift of 700–800 cm^{-1} on the $\pi \rightarrow \pi^*$ transition and a hypsochromic shift of 200–300 cm^{-1} on the $n \rightarrow \pi^*$ transition, accompanied by a 30% increase in the oscillator strength for both (I*a*) and (I*b*). As with the $\pi \rightarrow \pi^*$ transition, these results are in line with the observed effects: the positions of the corresponding absorption maxima in (I*a*) and (I*b*) are red-shifted by 900–1000 cm^{-1} with respect to the spectrum of a CCl_4 solution of (I) (Fig. 1). However, neither the difference in molecular geometry nor the intermolecular electrostatic

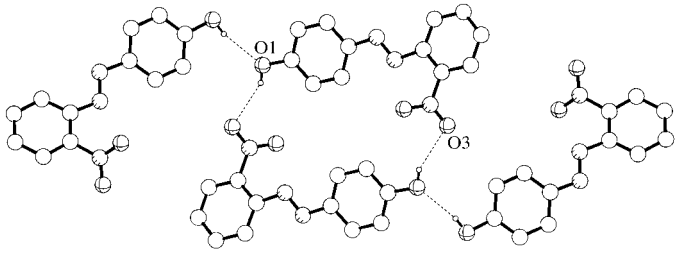

Figure 4
The hydrogen-bonded tetramer in (I*b*).

interactions explain the 1500 cm^{-1} red shift of the $n\pi^*$ band on transfer from solution to solid (I*a*) and (I*b*), or the increase in intensity of this band in (I*b*) with respect to (I*a*) (Fig. 1). Qualitatively, these effects can be explained by the mixing of the $n\pi^*$ excited state with intermolecular CT excitations. The *INDO-CISD* calculations on the inversion- and translation-related molecular dimers modelling the stacking in (I*a*) and (I*b*) partially confirm this supposition; in translation-related dimers, the $n \rightarrow \pi^*$ excitation is accompanied by some intermolecular CT (0.0003–0.0006 e) and the oscillator strength for this transition increases by 50% with respect to the isolated molecule, whereas for inversion-related dimers, the oscillator strength for this excitation decreases to a half of the original value. However, these calculations do not explain the observed red shift of the $n\pi^*$ absorption band, probably due to the fact that the methods based on the zero-differential-overlap approximation are not very well suited for reproducing intermolecular interactions.

Experimental

Compound (I) was prepared according to the established procedure of Elbs *et al.* (1924). Single crystals of (I*a*) and (I*b*) were grown by slow evaporation of chloroform and acetone solutions of (I), respectively. The powders prepared from the crystals of (I*a*) and (I*b*) were brown–yellow and orange, respectively. The UV–visible spectra were recorded on a Specord *M*-40 spectrophotometer (Carl Zeiss, Jena). Spectroscopic data: UV–visible [CCl_4, λ_{max}, nm (log ε)]: 350 (4.26), 433 (3.02). The *ab initio* calculations were performed with *GAMESS* (Schmidt *et al.*, 1993) using the 6-31G** basis set. Details of the calculations employing crystal electrostatic potential at the *AM*1 and *INDO* levels have been reported elsewhere (Yatsenko & Paseshnichenko, 2000).

Compound (I*a*)

Crystal data

$C_{12}H_9N_3O_3$
M_r = 243.22
Triclinic, $P\overline{1}$
a = 7.114 (2) Å
b = 7.380 (2) Å
c = 10.849 (4) Å
α = 96.68 (2)°
β = 97.49 (2)°
γ = 100.54 (2)°
V = 549.4 (3) Å^3
Z = 2
D_x = 1.470 Mg m^{-3}
Mo $K\alpha$ radiation
Cell parameters from 23 reflections
θ = 14.0–15.8°
μ = 0.11 mm^{-1}
T = 293 (2) K
Prism, yellow–brown
0.44 × 0.25 × 0.18 mm

Data collection

Enraf–Nonius CAD-4 diffractometer
Non-profiled ω scans
2395 measured reflections
2395 independent reflections
1599 reflections with $I > 2\sigma(I)$
θ_{max} = 27°
$h = -9 \rightarrow 8$
$k = -9 \rightarrow 9$
$l = 0 \rightarrow 13$
3 standard reflections
frequency: 80 min
intensity decay: none

Refinement

Refinement on F^2
$R[F^2 > 2\sigma(F^2)]$ = 0.038
$wR(F^2)$ = 0.101
S = 1.12
2395 reflections
199 parameters
All H-atom parameters refined
$w = 1/[\sigma^2(F_o^2) + (0.047P)^2]$ where $P = (F_o^2 + 2F_c^2)/3$
$(\Delta/\sigma)_{max}$ = 0.001
$\Delta\rho_{max}$ = 0.13 e Å^{-3}
$\Delta\rho_{min}$ = −0.13 e Å^{-3}

Compound (I*b*)

Crystal data

$C_{12}H_9N_3O_3$
M_r = 243.22
Monoclinic, $P2_1/n$
a = 3.8230 (10) Å
b = 23.014 (8) Å
c = 25.437 (9) Å
β = 92.73 (3)°
V = 2235.5 (13) Å^3
Z = 8
D_x = 1.445 Mg m^{-3}
Mo $K\alpha$ radiation
Cell parameters from 22 reflections
θ = 11.2–12.8°
μ = 0.11 mm^{-1}
T = 293 (2) K
Needle, orange
0.39 × 0.12 × 0.07 mm

Data collection

Enraf–Nonius CAD-4 diffractometer
Non-profiled ω scans
4574 measured reflections
3954 independent reflections
1544 reflections with $I > 2\sigma(I)$
R_{int} = 0.046
θ_{max} = 25°
$h = 0 \rightarrow 4$
$k = 0 \rightarrow 27$
$l = -30 \rightarrow 30$
3 standard reflections
frequency: 80 min
intensity decay: none

Refinement

Refinement on F^2
$R[F^2 > 2\sigma(F^2)]$ = 0.066
$wR(F^2)$ = 0.124
S = 0.98
3954 reflections
397 parameters
All H-atom parameters refined
$w = 1/[\sigma^2(F_o^2) + (0.032P)^2]$ where $P = (F_o^2 + 2F_c^2)/3$
$(\Delta/\sigma)_{max} < 0.001$
$\Delta\rho_{max}$ = 0.16 e Å^{-3}
$\Delta\rho_{min}$ = −0.15 e Å^{-3}

The range of refined C—H distances was 0.858 (15)–0.988 (15) Å in (I*a*) and 0.91 (4)–1.01 (3) Å in (I*b*).

Table 1
Selected geometric parameters (Å,°) for (I*a*) and (I*b*).

	(I*a*)	(I*b*) Molecule 1	(I*b*) Molecule 2
C4—N1—N2—C11	178.0 (1)	178.8 (4)	−179.6 (4)
O2···N2	2.726 (2)	2.788 (5)	2.771 (5)
Interplanar angles			
C1–C6/C4,N1,N2,C11	11.12 (9)	6.7 (3)	5.8 (3)
C4,N1,N2,C11/C11–C16	10.93 (9)	15.7 (3)	19.9 (3)
C1–C6/C11–C16	1.73 (9)	22.0 (3)	25.2 (3)
N3,O2,O3/C11–C16	38.44 (6)	51.6 (2)	51.0 (2)

Table 2
Hydrogen-bonding geometry (Å,°) for (I*a*) and (I*b*).

	D—H···*A*	*D*—H	H···*A*	*D*···*A*	*D*—H···*A*
(I*a*)	O1—H1···O2^{i}	0.96 (2)	1.93 (2)	2.879 (2)	174 (2)
(I*b*)	O1—H1···O3^{ii}	0.79 (5)	2.23 (5)	2.933 (5)	148 (5)
(I*b*)	O21—H21···O1^{iii}	0.79 (4)	2.10 (4)	2.866 (5)	164 (4)

Symmetry codes: (i) $-x, -y, 1-z$; (ii) $2-x, -y, 1-z$;(iii) $\frac{3}{2}-x, \frac{1}{2}+y, \frac{1}{2}-z$.

For both compounds, data collection: *CAD*-4 *Software* (Enraf–Nonius, 1989); cell refinement: *CAD*-4 *Software*; data reduction: *PROFIT* (Streltsov & Zavodnik, 1989); program(s) used to solve structure: *SHELXS*97 (Sheldrick, 1990); program(s) used to refine structure: *SHELXL*97 (Sheldrick, 1997). For compound (I*a*), molecular graphics: *ORTEP*-3 (Farrugia, 1997); for compound (I*b*), molecular graphics: *ORTEP*-3 and *PLUTON*92 (Spek, 1992). For both compounds, software used to prepare material for publication: *PARST* (Nardelli, 1983).

This work was supported in part by ICDD (grant No. 93-05).

Supplementary data for this paper are available from the IUCr electronic archives (Reference: NA1519). Services for accessing these data are described at the back of the journal.

References

Allen, F. H. & Kennard, O. (1993). *Chem. Des. Autom. News*, **8**, 1, 31–37.
Cromer, D. T., Lee, K.-Y. & Ryan, R. R. (1988). *Acta Cryst.* C**44**, 1673–1674.
Csikós, É., Ángyán, J. G., Böcskei, Z., Simon, K., Gönczi, C. & Hermecs, I. (1999). *Eur. J. Org. Chem.* pp. 2119–2125.
Dewar, M. J. S., Zoebish, E. G., Healy, E. F. & Stewart, J. J. P. (1985). *J. Am. Chem. Soc.* **107**, 3902–3909.
Dick, B. & Nickel, B. (1983). *Chem. Phys.* **78**, 1–16.
Elbs, K., Hirschel, O., Wagner, F., Himmler, K., Türk, W., Heinrich, A. & Lehmann, E. (1924). *J. Prakt. Chem.* **108**, 209–233.
Enraf–Nonius (1989). *CAD*-4 *Software*. Version 5.0. Enraf–Nonius, Delft, The Netherlands.
Farrugia, L. J. (1997). *J. Appl. Cryst.* **30**, 565.
Griffiths, J. (1976). *Color and Constitution of Organic Molecules*, p. 256. London: Academic Press.
Guillaumont, D. & Nakamura, S. (2000). *Dyes Pigm.* **46**, 85–92.
Hantzsch, A. (1907). *Z. Angew. Chem.* **20**, 1889.
Hoffmann, M., Schmidt, K., Fritz, T., Hasche, T., Agranovich, V. M. & Leo, K. (2000). *Chem. Phys.* **258**, 73–96.
Klebe, B., Graser, F., Hädicke, E. & Berndt, J. (1989). *Acta Cryst.* B**45**, 69–77.
Nardelli, M. (1983). *Comput. Chem.* **7**, 95–98.
Okawara, M., Kitao, T., Hirashima, T. & Matsuoka, M. (1988). *Organic Colorants: A Handbook of Data of Selected Dyes for Electro-Optical Applications*, pp. 72–75. Tokyo: Kodansha.
Philpott, M. R. (1971). *J. Chem. Phys.* **54**, 2120–2129.
Ridley, J. & Zerner, M. (1973). *Theor. Chim. Acta* (*Berlin*), **32**, 111–134.
Schmidt, M. W., Baldridge, K. K., Boatz, J. A., Elbert, S. T., Gordon, M. S., Jensen, J. H., Koseki, S., Matsunaga, N., Nguyen, S. A., Su, S. J., Windus, T. L., Dupuis, M. & Montgomery, J. A. (1993). *J. Comput. Chem.* **14**, 1347–1363.
Sebastian, L., Weiser, G. & Bässler, H. (1981). *Chem. Phys.* **61**, 125–135.
Sheldrick, G. M. (1990). *Acta Cryst.* A**46**, 467–473.
Sheldrick, G. M. (1997). *SHELXL*97. University of Göttingen, Germany.
Spek, A. L. (1992). *PLUTON*92. University of Utrecht, The Netherlands.
Streltsov, V. A. & Zavodnik, V. E. (1989). *Sov. Phys. Crystallogr.* **34**, 824–828.
Yatsenko, A. V., Chernyshev, V. V., Paseshnichenko, K. A. & Schenk, H. (2001). *Acta Cryst.* C**57**, 295–297.
Yatsenko, A. V. & Paseshnichenko, K. A. (2000). *Chem. Phys.* **262**, 293–301.